DOI: 10.1002/ejic.201100083

Temperature-Induced Enhancement of Catalytic Performance in Selective Hydrogen Generation from Hydrous Hydrazine with Ni-Based Nanocatalysts for Chemical Hydrogen Storage

Sanjay Kumar Singh,[a] Zhang-Hui Lu,[a] and Qiang Xu*[a]

Keywords: Nickel / Hydrogen / Hydrazine / Nanostructures / Temperature effects

We demonstrate here that Ni nanoparticles, which are inactive for the decomposition of hydrous hydrazine at room temperature, can exhibit drastically enhanced catalytic performance with an increase in reaction temperature to 323 K. At this reaction temperature, complete conversion of hydrous hydrazine with 100 % H_2 selectivity can be achieved by alloying Ni and Pt with a Pt content as low as 1 mol-%. This significant temperature effect coupled with the uniform alloy composition of Ni–Pt nanocatalysts results in the observed enhanced catalytic performance of the Ni–Pt nanocatalyst for hydrogen generation from hydrous hydrazine. In addition, evidence suggests that the Ni-based bimetallic catalysts can be used to release five equivalents of H_2 and one equivalent of N_2 from an aqueous solution of hydrazine borane $N_2H_4BH_3$.

Introduction

Development of new materials that can provide an alternative to fossil fuels for clean energy production, conversion, and storage is of paramount importance. Hydrogen has emerged as an alternative clean fuel, which produces only water when burning with oxygen or used in fuel cells.[1] However, safe and efficient hydrogen storage is one of the most difficult tasks on the path toward a hydrogen-energy-based society. However, despite extensive exploration over several decades, no single material investigated to date offers high volumetric and gravimetric hydrogen capacities, safe handling pressure and temperature, and effective recycling of byproducts.[1,2] Hydrous hydrazine, such as hydrazine monohydrate, $H_2NNH_2{\cdot}H_2O$, a liquid at room temperature,[3] has a hydrogen content available for hydrogen generation as high as 8.0 wt.-%, thus making it a promising candidate and safe in handling. Notably, nitrogen, the only byproduct produced in addition to hydrogen by hydrazine decomposition, can be transformed to ammonia by the Haber–Bosch process, homogeneous catalytic processes, or an electrolytic process;[4] and subsequently to hydrazine on a large scale,[5] or perhaps transformed directly to hydrazine by means of an electrolytic process similar to that for ammonia synthesis.[4c] Recent explorations in this direction have shown that hydrazine can be decomposed completely to hydrogen and nitrogen through Equation (1).[6–8]

$$H_2NNH_2 \rightarrow N_2 + 2H_2 \quad (1)$$

However, the key to exploit effectively the hydrogen-storage properties of hydrazine is to avoid its incomplete decomposition by an undesired reaction pathway [Equation (2)].

$$3H_2NNH_2 \rightarrow N_2 + 4NH_3 \quad (2)$$

A large number of metal catalysts have been investigated so far for the decomposition of hydrazine, and it has been shown that the reaction pathways for hydrazine decomposition strongly depend on the catalyst used and the reaction conditions.[6–10] However, the development of highly active, low-cost, and efficient catalysts is of significant importance for the practical use of hydrous hydrazine as a potential hydrogen-storage material.[7] Here, emphasis is placed on the development of suitable reaction conditions for hydrazine decomposition to hydrogen by using low-cost nanocatalysts such as Ni-based nanoparticles. We have observed that Ni nanoparticles/nanocrystallites, which are inactive for the decomposition of hydrous hydrazine at room temperature, can show drastically enhanced catalytic activity with an H_2 selectivity of 33% when the reaction temperature is raised to 323 K. This significant temperature effect can be suitably exploited to achieve 100 % H_2 selectivity at 323 K by alloying Ni and Pt with a Pt content as low as 1 mol-%. The present results indicate that a suitable reaction temperature may make it possible to achieve high catalytic performance for hydrogen generation by decomposition of hydrous hydrazine with Ni-based nanocatalysts with low content of noble metals.

[a] National Institute of Advanced Industrial Science and Technology (AIST),
Ikeda, Osaka, Japan
Fax: +81-72-751-7942
E-mail: q.xu@aist.go.jp

Supporting information for this article is available on the WWW under http://dx.doi.org/10.1002/ejic.201100083.

Results and Discussion

From our recent studies devoted to bimetallic-nanoparticle-catalyzed hydrous hydrazine conversion to hydrogen, nickel has emerged as a central component for all the active bimetallic catalysts.[7] However, in the past, we found that the monometallic Ni nanoparticles themselves are catalytically inactive for the decomposition of hydrous hydrazine at room temperature (298 K),[6] and therefore it is significantly important to make clear their activity in detail, for example, at various temperatures. Ni nanoparticles were prepared using our previously reported method;[6] their catalytic activity for hydrous hydrazine decomposition were examined at different reaction temperatures (298–343 K). In contrast to the catalytic inactivity of Ni nanoparticles at 298 K,[6,7] a significant enhancement in the catalytic performance of Ni nanoparticles for hydrous hydrazine decomposition has been observed with an increase in the reaction temperature. As shown in Figure 1, a release of 1.2 equiv. of gases was observed over 210 min at 323 K with monometallic Ni nanoparticles, which corresponds to an H_2 selectivity of 33%. However, no further increase in H_2 selectivity was observed at higher temperatures, whereas the reaction completion time was significantly reduced (i.e., 150 min at 333 K and 90 min at 343 K). From the volumetric observations, the overall reaction for the hydrogen decomposition over Ni nanoparticles can be expressed as [Equation (3)].[6]

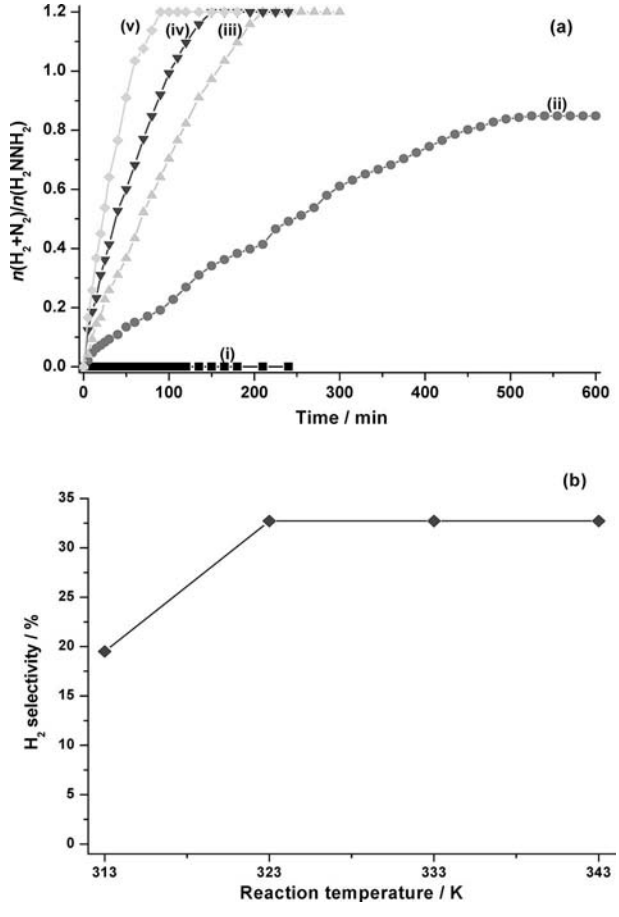

Figure 1. (a) Time-course plots of hydrogen generation by decomposition of hydrazine in aqueous solution (0.5 M) catalyzed by Ni nanoparticles (catalyst/H_2NNH_2 = 1:10) at the reaction temperatures of (i) 298, (ii) 313, (iii) 323, (iv) 333, and (v) 343 K. (b) Temperature dependence of H_2 selectivity from hydrous hydrazine decomposition catalyzed by Ni nanoparticles.

$$H_2NNH_2 \rightarrow 0.55N_2(g) + 0.66H_2(g) + 0.89NH_3 \quad (3)$$

Having established that the Ni nanoparticles are able to catalyze the hydrous hydrazine decomposition to hydrogen with a maximum of 33% H_2 selectivity by increasing the reaction temperature from room temperature to 323 K, we have extensively explored the effect of temperature on the catalytic performance of the Ni nanoparticles alloyed with a very low content of Pt. Bimetallic $Ni_{0.99}Pt_{0.01}$ nanoparticles were obtained by alloying Ni and Pt with a Pt content as low as 1 mol-% by using an aqueous-phase co-reduction process of the chloride salts of Ni^{2+} and Pt^{2+} in the presence of hexadecyltrimethyl ammonium bromide (CTAB). Catalytic decomposition reaction of hydrous hydrazine was initiated with the addition of hydrazine monohydrate into the reaction flask, and the relation between H_2 selectivity and the reaction temperature was studied by conducting the catalytic decomposition reaction of hydrous hydrazine in the temperature range of 298–333 K. At 323 K, a release of 3.0 equiv. of gas was observed in 120 min with the $Ni_{0.99}Pt_{0.01}$ nanocatalyst (Figure 2), which is in agreement with 100% selectivity for hydrogen and nitrogen according to Equation (1), thus indicating the complete decomposition of hydrazine into hydrogen and nitrogen in aqueous solution at 323 K. Moreover, the reaction completion time could be reduced to 70 min with 100% H_2 selectivity by increasing the reaction temperature from 323 to 333 K, whereas low H_2 selectivity and long reaction times were observed by decreasing the reaction temperatures to 313 K (88%, 5 h) or 298 K (80%, 7 h). Therefore, moderate temperatures are important for enhancing the catalytic performance of the bimetallic Ni–Pt nanocatalysts with low content of noble metals. It is worth noting that raising the reaction temperature to 323 K, only slightly higher than room temperature, makes it possible to achieve 100% H_2 selectivity for the Ni–Pt nanocatalyst with a Pt content as low as 1 mol-%, whereas at room temperature one needs to use a Ni–Pt nanocatalyst with much higher Pt content (7–34 mol-%) to achieve 100% H_2 selectivity.[7a]

Arrhenius treatment of the temperature-dependent rate data for hydrogen release from the decomposition of hydrous hydrazine in the presence of Ni and $Ni_{0.99}Pt_{0.01}$ nanocatalysts exhibits straight lines for both the catalysts (Figure S1 in the Supporting Information). The apparent activation energy (E_a) for hydrogen release from this reaction in the presence of bimetallic $Ni_{0.99}Pt_{0.01}$ nanocatalyst [$E_a \approx (49.95 \pm 5)$ kJ mol^{-1}] is significantly lower than that for the monometallic Ni nanocatalyst [$E_a \approx (81.08 \pm 5)$ kJ mol^{-1}]. The large difference in activation energy itself suggests a facile complete decomposition of hydrous hydrazine in the presence of $Ni_{0.99}Pt_{0.01}$ nanocatalyst. In contrast to the high activity of the $Ni_{0.99}Pt_{0.01}$ nanocatalyst, the effect of temperature does not introduce a significant enhancement in

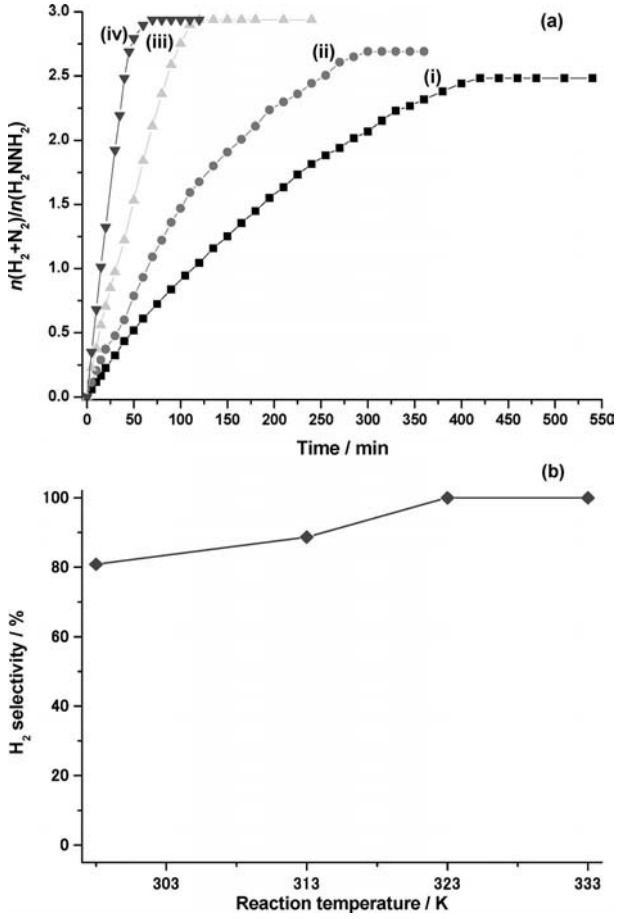

Figure 2. (a) Time-course plots for hydrogen generation by the decomposition of hydrazine in aqueous solution (0.5 M) catalyzed by $Ni_{0.99}Pt_{0.01}$ nanocatalyst (catalyst/H_2NNH_2 = 1:10) at the reaction temperatures of (i) 298, (ii) 313, (iii) 323, and (iv) 333 K. (b) Temperature dependence of H_2 selectivity from hydrous hydrazine decomposition catalyzed by $Ni_{0.99}Pt_{0.01}$ nanocatalyst.

the catalytic performance of Pt nanoparticles, which exhibit only around 7% H_2 selectivity at 323 K for hydrazine decomposition in aqueous solution (Figure 3). In comparison to the low H_2 selectivity observed for the monometallic Ni and Pt counterparts (around 33% and around 7% for Ni and Pt nanoparticles, respectively) at 323 K, the 100% H_2 selectivity exhibited by the $Ni_{0.99}Pt_{0.01}$ nanocatalyst suggested the involvement of the bimetallic phase as active centers on the catalyst surface, and that the significant interaction between Ni and Pt is necessary for the observed catalytic activity.[7a] The turnover frequency for the catalytic decomposition reaction of hydrazine in aqueous solution for $Ni_{0.99}Pt_{0.01}$ is 6 h^{-1} at 323 K, which is three times the value for $Ni_{0.93}Pt_{0.07}$ at 298 K.[7a] In addition, we have examined the activity and selectivity of the $Ni_{0.99}Pt_{0.01}$ for the decomposition of hydrazine in aqueous solution during repeated use and found no change in the H_2 selectivity (Figure S2 in the Supporting Information).

In addition, we have investigated the hydrogen-generation reaction from a mixture of hydrazine ($H_2NNH_2{\cdot}H_2O$) and ammonia borane (NH_3BH_3) (H_2NNH_2/NH_3BH_3 =

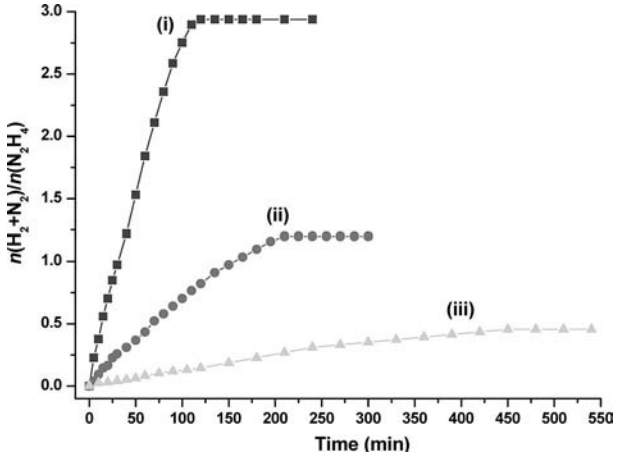

Figure 3. Time-course plots for hydrogen generation by the decomposition of hydrazine in aqueous solution (0.5 M) catalyzed by (i) $Ni_{0.99}Pt_{0.01}$, (ii) Ni, and (iii) Pt nanocatalysts (catalyst/H_2NNH_2 = 1:10) at 323 K.

1:1) in the presence of the $Ni_{0.99}Pt_{0.01}$ nanocatalyst [catalyst/(H_2NNH_2 + NH_3BH_3) = 1:10] at room temperature (298 K) and 323 K (Figure 4). A release of around 6.0 equiv. of gas from the mixture of hydrazine (1.0 equiv.) and ammonia borane (1.0 equiv.), which corresponds to $n(H_2 + N_2)/n(H_2NNH_2 + NH_3BH_3)$ = 3.0, at 323 K suggested the complete decomposition of hydrous hydrazine and hydrolysis of ammonia borane through the total reaction [Equation (4)].

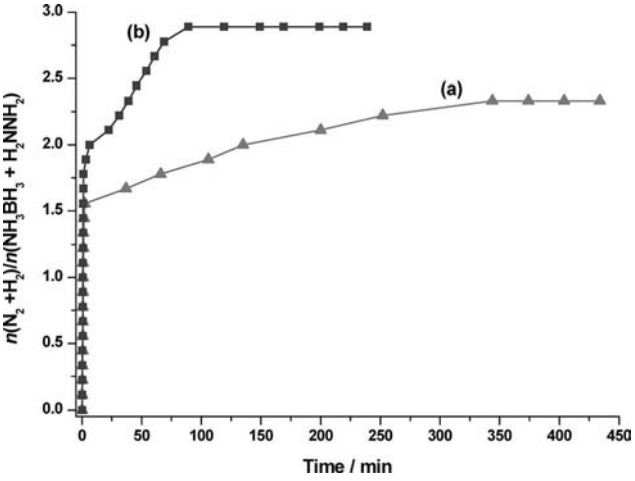

Figure 4. Time-course plots for hydrogen generation from a mixture of $H_2NNH_2{\cdot}H_2O$ (0.25 M) and NH_3BH_3 (0.25 M) (H_2NNH_2/NH_3BH_3 = 1:1) in aqueous solution in the presence of $Ni_{0.99}Pt_{0.01}$ nanocatalyst [catalyst/(H_2NNH_2 + NH_3BH_3) = 1:10] at (a) 298 and (b) 323 K.

$$H_2NNH_2 + NH_3BH_3 + 2H_2O \rightarrow N_2(g) + 5H_2(g) + NH_4^+ + BO_2^- \quad (4)$$

It is noteworthy that the hydrolysis of ammonia borane has fast kinetics in comparison with the decomposition of hydrazine over the Ni–Pt nanocatalyst. The present results suggest that an active catalyst such as the bimetallic Ni–Pt nanocatalysts can be used for the hydrogen release from

aqueous hydrazine boranes, for example [Equation (5)], which can release 6.0 equiv. of gas from hydrazine borane (HB).

$$H_2NNH_2BH_3 + 2H_2O \rightarrow N_2 + 5H_2 + HBO_2 \quad (5)$$

As it is reasonable to consider that the hydrolysis of the $-BH_3$ group in hydrazine boranes is relatively easy, a catalyst that can completely decompose hydrazine to N_2 and H_2 should be a key candidate for hydrogen release from aqueous hydrazine boranes as new hydrogen-storage materials.[11]

The X-ray photoelectron spectroscopic (XPS) analysis (Figure S3 in the Supporting Information) of Ni nanoparticles revealed that the Ni $2p_{3/2}$ and Ni $2p_{1/2}$ core levels show binding energies of 853.59 and 870.80 eV, respectively.[12] A peak that appeared at 858.16 eV, assigned to the oxide of Ni, could be readily removed by 36 min of argon sputtering. The powder X-ray diffraction (XRD; Figure S4 in the Supporting Information) data illustrates the crystalline nature of Ni nanoparticles, in which the major diffraction peak at the 2θ value of 45.38° can be indexed to the (111) diffraction plane of face-centered cubic (*fcc*) unit cell of Ni (PDF #65-0380). Consistent with the analogous XPS and XRD analysis results, SEM images (Figure S5 in the Supporting Information) of Ni nanoparticles before and after the reaction suggest a slight aggregation of Ni nanoparticles during the catalytic reaction at 323 K. The Brunauer–Emmett–Teller (BET) surface areas (Figure S6 in the Supporting Information) of the Ni nanoparticles before and after the reaction are 47.8 and 28.4 $m^2 g^{-1}$, respectively. Transmission electron microscopic (TEM) images of the Ni nanoparticles after the reaction show an average particle size of around 5 nm (Figure 5). High-angle annular dark-field scanning TEM (HAADF-STEM) along with energy-dispersed X-ray spectroscopic (EDS) analysis from several points of the Ni nanoparticles reveals the presence of nickel element (see Figure S7 in the Supporting Information). The selected area electron diffraction (SAED) measurements suggest the crystalline nature of the Ni nanoparticles (Figure 5).

XPS, TEM, and EDS measurements were performed for the $Ni_{0.99}Pt_{0.01}$ nanocatalyst. The XPS analysis (Figure S8 in the Supporting Information) of $Ni_{0.99}Pt_{0.01}$ nanocatalysts reveals that the Ni $2p_{3/2}$ and $2p_{1/2}$ core levels show binding energies of 853.28 and 870.48 eV, respectively, whereas the Pt $4f_{7/2}$ and $4f_{5/2}$ core levels show binding energies of 71.44 and 75.16 eV, respectively.[12] A thin oxide cover, presumably formed during exposure to air, was observed, which can be readily removed by argon sputtering. Consistent with other Ni–Pt compositions, the Pt $4f_{7/2}$ core level for the $Ni_{0.99}Pt_{0.01}$ nanocatalyst shifts to a higher binding energy than that for the monometallic Pt (Pt $4f_{7/2}$ 70.9 eV).[12] Argon-sputtering experiments over a period of 0 to 186 min for the $Ni_{0.99}Pt_{0.01}$ nanocatalyst confirmed the uniform distribution of Ni and Pt atoms in the nanoparticle with an alloy composition. The powder XRD profile (Figure S9 in the Supporting Information) of $Ni_{0.99}Pt_{0.01}$ nanocatalyst shows a face-centered cubic (*fcc*) diffraction pattern with a major peak at 2θ value of 44.56°. The observed XRD diffraction pattern is analogous to that of the (111) plane for nickel and is consistent with other Ni–Pt alloy nanocatalysts with higher nickel content.

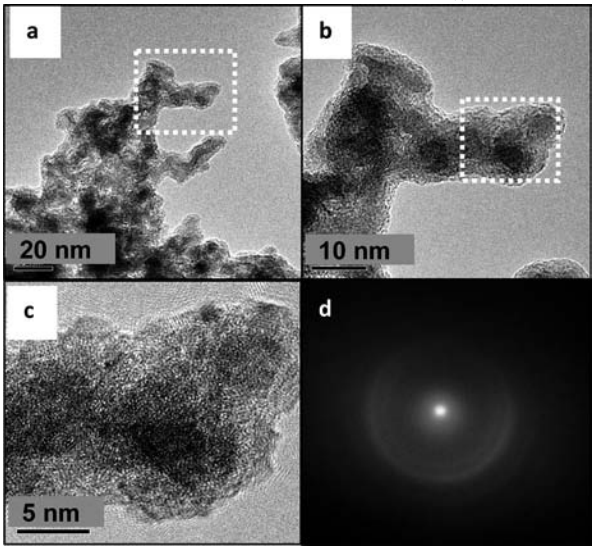

Figure 5. (a–c) TEM images at different magnifications [scale bar (a) 20, (b) 10, and (c) 5 nm] with (d) corresponding SAED pattern of Ni nanoparticles after the hydrazine decomposition reaction in aqueous solution at 323 K.

TEM and HRTEM images for $Ni_{0.99}Pt_{0.01}$ nanocatalysts shown in Figure 6 reveal the presence of partially aggregated nanoparticles of irregular shape with an average particle size of around 5 nm and are consistent with the previous observations with Ni–Pt nanoparticles for which the nanoparticle size is independent of the composition of Ni–Pt nanocatalysts.[7a] In addition, the TEM observations (Figure 6) of the $Ni_{0.99}Pt_{0.01}$ nanocatalysts before and after the reaction show no appreciable change in particle size (around 5 nm). HAADF-STEM measurements along with EDS analysis from several points of the nanoparticles reveal the presence of both Ni and Pt elements (Figures S10 and S11 in the Supporting Information). The SAED measurements suggest the crystalline nature of the $Ni_{0.99}Pt_{0.01}$ nanocatalysts (Figure 6). The BET surface area of $Ni_{0.99}Pt_{0.01}$ is 50.03 $m^2 g^{-1}$.

The release of around 1.2 equiv. of gas from the hydrazine decomposition at 323 K, which corresponds to a H_2 selectivity of 33%, suggests that the catalyst surface of Ni nanoparticles activates the hydrazine decomposition through both the reaction pathways in Equations (1) and (2) simultaneously. One can understand that the bonding pattern and stability of the different adsorbed species of the reactant on the catalyst surface are key factors that determine the performance of a catalyst. However, the mobility and chances of the interaction of the reactant to the catalyst can be enhanced with the increase in the reaction temperature. As the electronic and structural properties of the surface of the catalysts are significantly tuned with the introduction of a second component, a bimetallic catalyst might exhibit enhanced activity to those of the corresponding mo-

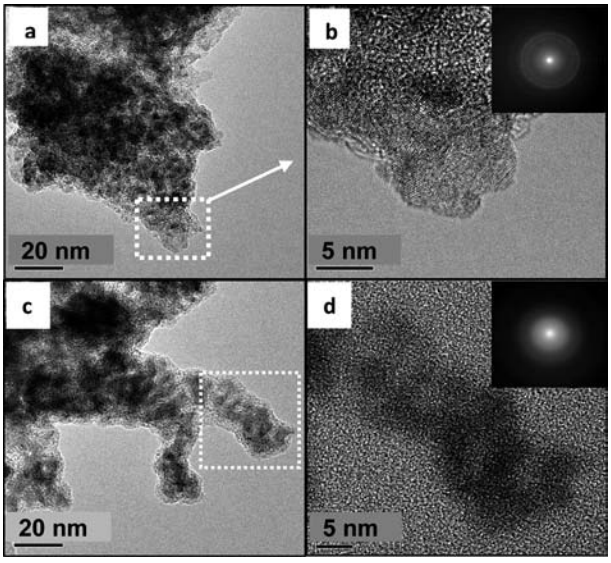

Figure 6. (a,c) TEM and (b,d) HRTEM images with corresponding (inset) SAED patterns of $Ni_{0.99}Pt_{0.01}$ nanocatalysts (a,b) before and (c,d) after the hydrazine decomposition reaction in aqueous solution at 323 K.

nometallic components.[13] The significant temperature effect, which led to a drastic enhancement of the catalytic performance of Ni nanoparticles, has been extended to the Ni–Pt alloy nanocatalysts. A 100% H_2 selectivity for the decomposition of hydrous hydrazine has been achieved with $Ni_{0.99}Pt_{0.01}$ nanocatalysts, which have a Pt content as low as 1 mol-%. Considering the uniform composition of the $Ni_{0.99}Pt_{0.01}$ nanocatalyst, which indicates the co-existence of bimetallic phase on the active sites of the catalyst surface, and the temperature effect, the observed 100% H_2 selectivity exhibited by the $Ni_{0.99}Pt_{0.01}$ nanocatalyst results from the activation of hydrazine bonds towards its complete decomposition for selective release of hydrogen and nitrogen through decomposition reaction pathway in Equation (1).

Conclusion

We have demonstrated that the catalytic performance of the Ni nanoparticles for the decomposition of hydrazine in aqueous solution can be enhanced appreciably from inactive at 298 K to active with around 33% H_2 selectivity at 323 K. Furthermore, this significant temperature effect has also been applied to bimetallic Ni–Pt nanocatalysts, which were prepared by alloying Ni and Pt with a Pt content as low as 1 mol-%, and for which the temperature effect coupled with the uniform alloy composition of the bimetallic Ni–Pt phase results in 100% H_2 selectivity from catalytic decomposition of hydrazine in aqueous solution at 323 K. The present system, which includes much lower Pt content, shows promise in the development of low-cost, high-performance catalysts for the decomposition of hydrazine to hydrogen. We believe that in combination with our process for highly efficient catalytic decomposition of hydrous hydrazine to hydrogen, an energy-efficient recycling of the by-product N_2 to hydrazine by an electrolytic process, similar to that for ammonia synthesis,[4c] could significantly enhance the practical application of hydrous hydrazine as a highly promising hydrogen-storage material.

Experimental Section

Commercial chemicals were used as received for catalyst preparation and hydrazine decomposition experiments. Hydrazine monohydrate ($H_2NNH_2{\cdot}H_2O$, 99%), sodium borohydride ($NaBH_4$, 99%), and hexadecyltrimethyl ammonium bromide (CTAB, 95%) were obtained from Aldrich. Ammonia borane (NH_3BH_3, 97%) was purchased from AVIABOR. Potassium tetrachloroplatinate(II) (K_2PtCl_4, 99.9%) and nickel chloride hexahydrate ($NiCl_2{\cdot}6H_2O$, 99.9%) were obtained from Wako. Powder X-ray diffraction (XRD) studies were performed with a Rigaku RINT-2000 X-ray diffractometer (Cu-K_α). A scanning electron microscope (SEM, Hitachi S-5000) and transmission electron microscope (TEM, FEI TECNAI G_2) equipped with selected area electron diffraction (SAED) and energy dispersed X-ray detector (EDS) were used to collect the detailed microstructure information. The SEM and TEM samples were prepared by depositing few droplets of the nanoparticle suspension onto amorphous carbon-coated copper grids, which were dried under an argon atmosphere. The surface-area measurements were performed by N_2 adsorption at liquid N_2 temperature with automatic volumetric adsorption equipment (Belsorp II). XPS analysis was carried out with a Shimadzu ESCA-3400 X-ray photoelectron spectrometer using an Mg-K_α source (10 kV, 10 mA). The Ar-sputtering experiments were carried out under the conditions of background vacuum 3.2×10^{-6} Pa, sputtering acceleration voltage 1 kV.

Preparation of the Monometallic Ni Nanocatalyst: An aqueous solution (1.5 mL) of $NaBH_4$ (0.020 g, 0.526 mmol) was added dropwise to an aqueous suspension (2.5 mL) of $NiCl_2{\cdot}6H_2O$ (0.047 g, 0.02 mmol) and CTAB (0.050 g, 0.142 mmol), obtained by sonication and stirring for 5 min. The content of the flask was vigorously shaken for 2 min, thereby resulting in the generation of Ni nanoparticles as a black suspension, which was used as prepared for the catalytic reaction.

Preparation of the Monometallic Pt Nanocatalyst: An analogous synthetic procedure as for the Ni nanoparticles was adapted. K_2PtCl_4 (0.083 g, 0.02 mmol) was used instead of $NiCl_2{\cdot}6H_2O$.

Preparation of the $Ni_{0.99}Pt_{0.01}$ Nanocatalyst: $Ni_{0.99}Pt_{0.01}$ nanoparticles were prepared following a surfactant-aided co-reduction process analogous to that reported previously.[7a] In brief, an aqueous suspension that contained $NiCl_2{\cdot}6H_2O$ and K_2PtCl_4 in 99:1 molar ratio was co-reduced by using an aqueous solution of $NaBH_4$ in the presence of CTAB, thereby resulting in the generation of $Ni_{0.99}Pt_{0.01}$ nanocatalyst as a black suspension, which was used as prepared for the catalytic reaction.

Catalytic Reaction for Hydrogen Release from Hydrous Hydrazine: Catalytic reactions were carried out at room temperature and elevated temperatures using a two-necked, round-bottomed flask with one of the flask openings connected to a gas burette and another used for the introduction of hydrazine monohydrate. Catalytic decomposition reaction of hydrazine for the release of hydrogen (along with nitrogen) was initiated by stirring the mixture of hydrazine monohydrate (0.1 mL, 1.97 mmol), which was introduced with a syringe to the reaction flask that contained the aqueous suspension (4.0 mL) of the as-prepared nanocatalysts (catalyst/H_2NNH_2 = 1:10; prepared as described above). The gases released

during the reaction were passed through a trap that contained hydrochloric acid (1.0 M) to ensure the absorption of ammonia, if produced, the volume of which was monitored using the gas burette. Catalyst-stability experiments were conducted over the same catalyst by adding an additional equivalent amount of $N_2H_4{\cdot}H_2O$ to the reaction vessel after the completion of previous catalytic run.

Catalytic Reaction for Hydrogen Release from a Mixture of Hydrazine and Ammonia Borane: An experimental arrangement analogous to that with catalytic hydrazine decomposition was used for this reaction also by using a mixture of hydrazine monohydrate (0.05 mL) and ammonia borane (0.031 g) in 1:1 molar ratio and the as-prepared $Ni_{0.99}Pt_{0.01}$ nanocatalyst [catalyst/(H_2NNH_2 + NH_3BH_3) = 1:10] at 298 and 323 K.

Characterization of Nanocatalysts: Nanocatalysts were collected by centrifugation (15000 rpm, 10 min, 298 K) from the reaction mixture (before and after the catalytic reaction). They were washed twice with water and ethanol (5.0 mL), dried at 373 K for 8 h, and then used for SEM, TEM, XPS, and powder XRD measurements.

Supporting Information (see footnote on the first page of this article): Experimental results of the catalytic reactions and XPS, XRD, SEM, and TEM results for nanoparticles.

Acknowledgments

We acknowledge the financial support from the Japan Society for the Promotion of Science (JSPS) and the National Institute of Advanced Industrial Science and Technology (AIST), Japan. S. K. S. thanks JSPS for a postdoctoral fellowship.

[1] a) A. Staubitz, A. P. M. Robertson, I. Manners, *Chem. Rev.* **2010**, *110*, 4079–4124; b) H.-L. Jiang, S. K. Singh, J.-M. Yan, X.-B. Zhang, Q. Xu, *ChemSusChem* **2010**, *3*, 541–549; c) J. Graetz, *Chem. Soc. Rev.* **2009**, *38*, 73–82; d) Z. Xiong, C. K. Yong, G. Wu, P. Chen, W. Shaw, A. Karkamkar, T. Autrey, M. O. Jones, S. R. Johnson, P. P. Edwards, W. I. F. David, *Nat. Mater.* **2007**, *7*, 138–141; e) F. H. Stephens, V. Pons, R. T. Baker, *Dalton Trans.* **2007**, 2613–2626; f) H. V. K. Diyabalanage, T. Nakagawa, R. P. Shrestha, T. A. Semelsberger, B. L. Davis, B. L. Scott, A. K. Burrell, W. I. F. David, K. R. Ryan, M. O. Jones, P. P. Edwards, *J. Am. Chem. Soc.* **2010**, *132*, 11836–11837.

[2] a) B. Loges, A. Boddien, H. Junge, M. Beller, *Angew. Chem. Int. Ed.* **2008**, *47*, 3962–3965; b) M. Chandra, Q. Xu, *J. Power Sources* **2006**, *156*, 190–194; c) Q. Xu, M. Chandra, *J. Power Sources* **2006**, *163*, 364–370; d) G. A. Deluga, J. R. Salge, L. D. Schmidt, X. E. Verykios, *Science* **2004**, *303*, 993–997; e) N. L. Rosi, J. Eckert, M. Eddaoudi, D. T. Vodak, J. Kim, M. O'Keeffe, O. M. Yaghi, *Science* **2003**, *300*, 1127–1129.

[3] E. W. Schmidt, *Hydrazine and its Derivatives: Preparation, Properties, Applications*, 2nd ed., Wiley, New York, **1984**.

[4] a) N. Hazari, *Chem. Soc. Rev.* **2010**, *39*, 4044–4056; b) J. M. Chin, R. R. Schrock, P. Müller, *Inorg. Chem.* **2010**, *49*, 7906–7916; c) T. Murakami, T. Nishikiori, T. Nohira, Y. Ito, *J. Am. Chem. Soc.* **2003**, *125*, 334–335; d) V. Smil, *Enriching the Earth: Fritz Haber, Carl Bosch and the Transformation of World Food Production*, MIT Press, Cambridge, MA, **2004**.

[5] a) S. Sridhar, T. Srinivasan, U. Virendra, A. A. Khan, *Chem. Eng. J.* **2003**, *94*, 51–56; b) H. Hayashi, *Res. Chem. Intermed.* **1998**, *24*, 183–196; c) H. Hayashi, *Catal. Rev.* **1990**, *32*, 229–277.

[6] S. K. Singh, X.-B. Zhang, Q. Xu, *J. Am. Chem. Soc.* **2009**, *131*, 9894–9895.

[7] a) S. K. Singh, Q. Xu, *Inorg. Chem.* **2010**, *49*, 6148–6152; b) S. K. Singh, Q. Xu, *Chem. Commun.* **2010**, *46*, 6545–6547; c) S. K. Singh, Q. Xu, *J. Am. Chem. Soc.* **2009**, *131*, 18032–18033.

[8] a) H. Gu, R. Ran, W. Zhou, Z. Shao, W. Jin, N. Xu, J. Ahn, *J. Power Sources* **2008**, *177*, 323–329; b) S. J. Cho, J. Lee, Y. S. Lee, D. P. Kim, *Catal. Lett.* **2006**, *109*, 181–187; c) M. Zheng, R. Cheng, X. Chen, N. Li, L. Li, X. Wang, T. Zhang, *Int. J. Hydrogen Energy* **2005**, *30*, 1081–1089; d) X. Chen, T. Zhang, M. Zheng, Z. Wu, W. Wu, C. Li, *J. Catal.* **2004**, *224*, 473–478; e) W. E. Armstrong, L. B. Ryland, H. H. Voge, US Patent **1978**, 4,124,538.

[9] a) J. B. O. Santos, G. P. Valença, J. A. J. Rodrigues, *J. Catal.* **2002**, *210*, 1–6; b) J. E. de Medeiros, G. P. Valença, *Braz. J. Chem. Eng.* **1998**, *15*, 126–131.

[10] D. J. Alberas, J. Kiss, Z.-M. Liu, J. M. White, *Surf. Sci.* **1992**, *278*, 51–61.

[11] a) H.-L. Jiang, Q. Xu, *Catal. Today* **2010**, DOI: 10.1016/j.cattod.2010.09.019; b) T. Hügle, M. F. Kühnel, D. Lentz, *J. Am. Chem. Soc.* **2009**, *131*, 7444–7446; c) N. Vinh-Son, S. Swinnen, M. H. Matus, M. T. Nguyen, D. A. Dixon, *Phys. Chem. Chem. Phys.* **2009**, *11*, 6339–6344.

[12] J. F. Moulder, W. F. Stickle, P. E. Sobol, K. D. Bomben, *Handbook of X-ray Photoelectron Spectroscopy: A Reference Book of Standard Spectra for Identification and Interpretation of XPS Data*, Physical Electronics, Eden Prairie, MN, **1995**.

[13] a) J. Greeley, I. E. L. Stephens, A. S. Bondarenko, T. P. Johansson, H. A. Hansen, T. F. Jaramillo, J. Rossmeisl, I. Chorkendorff, J. K. Nørskov, *Nat. Chem.* **2009**, *1*, 552–556; b) R. Ferrando, J. Jellinek, R. L. Johnston, *Chem. Rev.* **2008**, *108*, 845–910; c) V. R. Stamenkovic, B. S. Mun, M. Arenz, K. J. J. Mayrhofer, C. A. Lucas, G. Wang, P. N. Ross, N. M. Markovic, *Nat. Mater.* **2007**, *6*, 241–247; d) J. Greeley, M. Mavrikakis, *Nat. Mater.* **2004**, *3*, 810–815.

Received: January 24, 2011
Published Online: March 29, 2011

